

DETERMINING MASSES OF SUPERSYMMETRIC PARTICLES

B. K. Gjelsten¹, D. J. Miller², P. Osland³

¹ Laboratory for High Energy Physics, University of Bern, CH-3012 Bern, Switzerland

² Department of Physics and Astronomy, University of Glasgow, Glasgow G12 8QQ, U.K.

³ Department of Physics, University of Bergen, N-5007 Bergen, Norway

Abstract. *If supersymmetric particles are produced at the Large Hadron Collider it becomes very important not only to identify them, but also to determine their masses with the highest possible precision, since this may lead to an understanding of the SUSY-breaking mechanism and the physics at some higher scale. We here report on studies of how such mass measurements are obtained, and how the precision can be optimized.*

Key words: *SUSY, BSM, MSSM*

1. INTRODUCTION

Supersymmetry [1] has attracted a lot of attention as a natural extension of the Standard Model of particle physics. Not only does it solve the hierarchy problem, it also has many other attractive features, the most celebrated of which are that it provides a *natural* mechanism for generating the Higgs potential which breaks the electroweak symmetry [2] and that it supplies a good candidate for cold dark matter [3]. Furthermore, if it is to be relevant in solving the hierarchy problem it must exhibit experimental consequences at the TeV-scale, and therefore can be tested by experiments at the Large Hadron Collider (LHC).

If supersymmetric particles are produced at the LHC, it will become important to identify them and accurately measure their masses. Only an accurate determination of the supersymmetric particle masses and couplings will allow us to determine the low energy soft supersymmetry breaking parameters. It is hoped that extrapolation of these masses and couplings to

Presented at the *Southeastern European Workshop Challenges Beyond the Standard Model*, 19-23 May 2005, Vrnjacka Banja, Serbia

high energies will provide an insight into the mechanism of supersymmetry breaking and, more generally, physics at the GUT scale [4].

Here we will discuss supersymmetric mass measurements with reference to one particular model of supersymmetry breaking, minimal super-gravity (mSUGRA) [2, 5]. In this model, the supersymmetry is broken by the interaction of new particles at high energy which are only linked to the usual particles by gravitational interactions; this new sector of physics is often referred to as the *hidden sector*. At the GUT scale, the scalar supersymmetric particles are assumed to have a common mass, m_0 , while the gauginos have a common mass $m_{1/2}$. The trilinear couplings are also taken to be universal at the GUT scale and denoted A_0 .

Furthermore, in this model R-parity is conserved. Thus, supersymmetric particles are produced in pairs, and the lightest one (from each decay chain) escapes detection. While this provides a very distinctive *missing energy* signature, it complicates the measuring of masses at the LHC since decays cannot be fully reconstructed.

Instead, mass measurements rely on continuous mass distributions of decay products which attain extrema for certain configurations of the particle momenta that are unambiguously determined by the masses of initial, intermediate and final particles involved. These relations may often be inverted to give the masses of unstable particles.

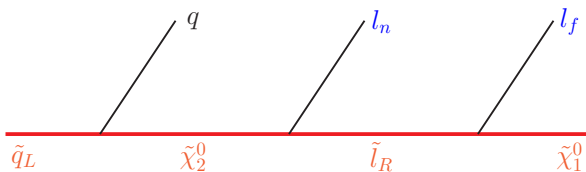


Figure 1: Typical cascade decay chain.

We here report on how supersymmetric mass measurements can be made [6, 7] by examining the mass distribution endpoints or ‘edges’ of the long decay chains (see Fig. 1)

$$\tilde{q} \rightarrow \tilde{\chi}_2^0 q \rightarrow \tilde{l}_n q \rightarrow \tilde{\chi}_1^0 l_n q \quad (1)$$

and

$$\tilde{g} \rightarrow \tilde{q} q_n \rightarrow \tilde{\chi}_2^0 q_f q_n \rightarrow \tilde{l}_n q_f q_n \rightarrow \tilde{\chi}_1^0 l_n q_f q_n, \quad (2)$$

where \tilde{g} denotes the gluino, \tilde{q} a squark, \tilde{l} a slepton, whereas $\tilde{\chi}_2^0$ and $\tilde{\chi}_1^0$ are the two lightest neutralinos. For easier reference a subscript is given to the quarks and leptons when needed (“n” for “near” and “f” for “far”).

For the decay chain (1) the following four invariants can be defined:

$$m_{ll}, \quad m_{ql_n}, \quad m_{ql_f}, \quad m_{qll}, \quad (3)$$

where the subscripts are left out when there is no ambiguity. For the longer chain (2) seven more invariants can be defined, but for simplicity we will here keep mostly to the first case, as adding the gluino in any case involves no additional complications on the conceptual level.

2. INVARIANT MASS DISTRIBUTIONS

In practice, one will usually not be able to distinguish the “near” and the “far” leptons of Fig. 1 and Eq. (3). Therefore, two alternative distributions are defined:

$$m_{ql(\text{low})} = \min(m_{ql_n}, m_{ql_f}), \quad m_{ql(\text{high})} = \max(m_{ql_n}, m_{ql_f}). \quad (4)$$

For the Snowmass mSUGRA benchmark point SPS 1a (α) [8, 6], the electroweak-scale masses are given as

$$\{m_{\tilde{q}_L}, m_{\tilde{\chi}_2^0}, m_{\tilde{l}_R}, m_{\tilde{\chi}_1^0}\} = \{537.2, 176.8, 143.0, 96.1\} \text{ GeV}. \quad (5)$$

For these mass values, the invariant distributions for

$$m_{ll}, \quad m_{ql(\text{low})}, \quad m_{ql(\text{high})}, \quad m_{qll} \quad (6)$$

are given in Fig. 2. For comparison, we also show the corresponding distributions for the point SPS 1a (β) [6], a related mass scenario, also on the SPS 1a line [8], for which the masses are

$$\{m_{\tilde{q}_L}, m_{\tilde{\chi}_2^0}, m_{\tilde{l}_R}, m_{\tilde{\chi}_1^0}\} = \{826.3, 299.1, 221.9, 161.0\} \text{ GeV}, \quad (7)$$

We see that while the dilepton mass distribution has a simple triangular shape, and $m_{ql(\text{low})}$ for SPS 1a has a smooth rounded shape, the other distributions have several abrupt changes in slope. The reason for this is that they are composite, with different functions describing the different intervals. In fact, these functions have recently been worked out analytically [9]. The great variety of these functional forms represents a complication to the experimental determination of the over-all endpoints.

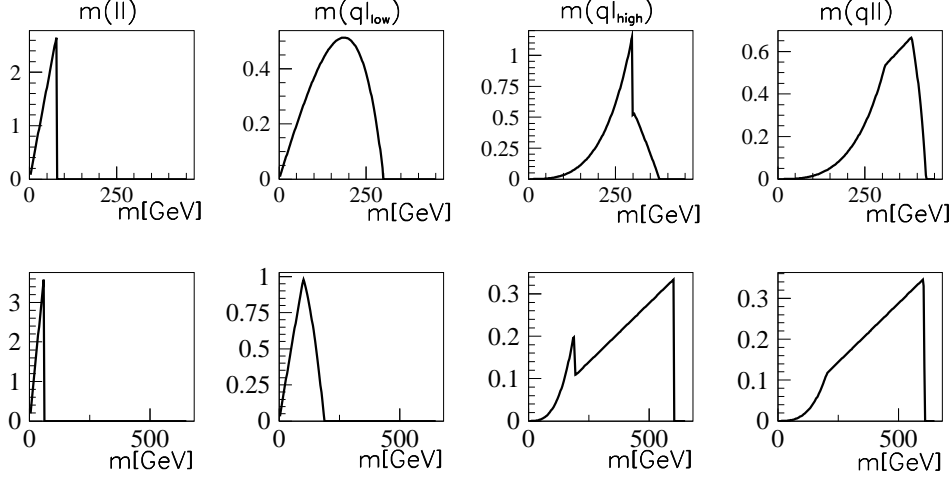


Figure 2: Invariant mass distributions for the SPS 1a (α) [8, 6] (upper row) and SPS 1a (β) [6] (lower row) benchmark points.

Most of the endpoints are given by composite functions with different expressions for different mass constellations. For example, the endpoints of $m_{ql(\text{low})}^{\text{max}}$ and $m_{ql(\text{high})}^{\text{max}}$ are given by [10, 6]:

$$(m_{ql(\text{low})}^{\text{max}}, m_{ql(\text{high})}^{\text{max}}) = \left\{ \begin{array}{ll} (m_{ql_n}^{\text{max}}, m_{ql_f}^{\text{max}}) & \text{for Case 1} \\ (m_{ql(\text{eq})}^{\text{max}}, m_{ql_f}^{\text{max}}) & \text{for Case 2} \\ (m_{ql(\text{eq})}^{\text{max}}, m_{ql_n}^{\text{max}}) & \text{for Case 3} \end{array} \right\} \quad (8)$$

with

$$\begin{aligned} (m_{ql_n}^{\text{max}})^2 &= (m_{\tilde{q}_L}^2 - m_{\tilde{\chi}_2^0}^2)(m_{\tilde{\chi}_2^0}^2 - m_{\tilde{l}_R}^2)/m_{\tilde{\chi}_2^0}^2 \\ (m_{ql_f}^{\text{max}})^2 &= (m_{\tilde{q}_L}^2 - m_{\tilde{\chi}_2^0}^2)(m_{\tilde{l}_R}^2 - m_{\tilde{\chi}_1^0}^2)/m_{\tilde{l}_R}^2 \\ (m_{ql(\text{eq})}^{\text{max}})^2 &= (m_{\tilde{q}_L}^2 - m_{\tilde{\chi}_2^0}^2)(m_{\tilde{l}_R}^2 - m_{\tilde{\chi}_1^0}^2)/(2m_{\tilde{l}_R}^2 - m_{\tilde{\chi}_1^0}^2) \end{aligned} \quad (9)$$

and the different cases given by the linear and quadratic ratios of the underlying (unknown) masses:

$$\text{Case 1: } \quad 2m_{\tilde{l}_R}^2 > m_{\tilde{\chi}_1^0}^2 + m_{\tilde{\chi}_2^0}^2 > 2m_{\tilde{\chi}_1^0}m_{\tilde{\chi}_2^0}$$

$$\begin{aligned}
\text{Case 2 : } & m_{\tilde{\chi}_1^0}^2 + m_{\tilde{\chi}_2^0}^2 > 2m_{\tilde{l}_R}^2 > 2m_{\tilde{\chi}_1^0}m_{\tilde{\chi}_2^0} \\
\text{Case 3 : } & m_{\tilde{\chi}_1^0}^2 + m_{\tilde{\chi}_2^0}^2 > 2m_{\tilde{\chi}_1^0}m_{\tilde{\chi}_2^0} > 2m_{\tilde{l}_R}^2
\end{aligned}
\tag{10}$$

These methods for determining the masses of supersymmetric particles have been extensively studied in the past [11]. Our studies [6, 7, 12] extend the earlier works by (i) discussing theoretical distributions which arise for different mass scenarios (examples are shown in Fig. 2), (ii) providing inversion formulas (by using the endpoints of the four distributions (6) the edge formulas can be solved for the masses $m_{\tilde{q}_L}$, $m_{\tilde{l}_R}$, $m_{\tilde{\chi}_2^0}$ and $m_{\tilde{\chi}_1^0}$), (iii) discussing ambiguities and complications related to the composite nature of the endpoint expressions, (iv) extension of the method to include a gluino at the head of the chain.

3. RESULTS

In order to estimate the precision that may be obtained at the LHC, for the actual masses $m_{\tilde{g}}$, $m_{\tilde{q}_L}$, $m_{\tilde{l}_R}$, $m_{\tilde{\chi}_2^0}$ and $m_{\tilde{\chi}_1^0}$, we have investigated the decay chains (1) and (2) for two mass scenarios, SPS 1a (α) of Eq. (5) and SPS 1a (β) of Eq. (7).

The latter has higher masses. This would be an advantage for the kinematics, but higher masses also lead to lower cross sections, and thus a signal more easily masked by the background. The simulation was performed using the Monte Carlo program PYTHIA 6.2 [13], and the events were then passed through ATLFast [14], a simulation of the ATLAS detector.

A critical issue in this kind of analysis is the background. The Standard Model background can to a large extent be removed, it turns out, by exploiting the fact that the two leptons must be of the same flavour. In most cases, the SM background events which mimic the signal, such as $t\bar{t} \rightarrow b\bar{b}W^+W^- \rightarrow b\bar{b}l^+l^-\nu\bar{\nu}$ produce as many different-flavour lepton pairs ($e^\pm\mu^\mp$) as same-flavour lepton pairs (e^+e^- , $\mu^+\mu^-$)². Since these two background selections are statistically identical, the same-flavour part, which is collected together with the signal, can be removed statistically by subtracting the different-flavour part. Other SUSY decays will however contribute background events that are harder to control. The considered squark (or gluino) will typically be produced in association with another squark or gluino, which gives rise to a similar decay chain. This leads most importantly to an additional hard jet. (We make here the usual assumption that the mass difference between the squarks and the sparticles into which they

²Taus are not used because of their bad experimental resolution.

decay is large, producing on average the hardest jets in the event.) As it is not possible to know which of the two leading jets belongs to the signal, one will in principle select the incorrect jet in half of the cases or more. This adds considerably to the background and is the main reason why the experimental distributions tend to differ noticeably from the original distributions.

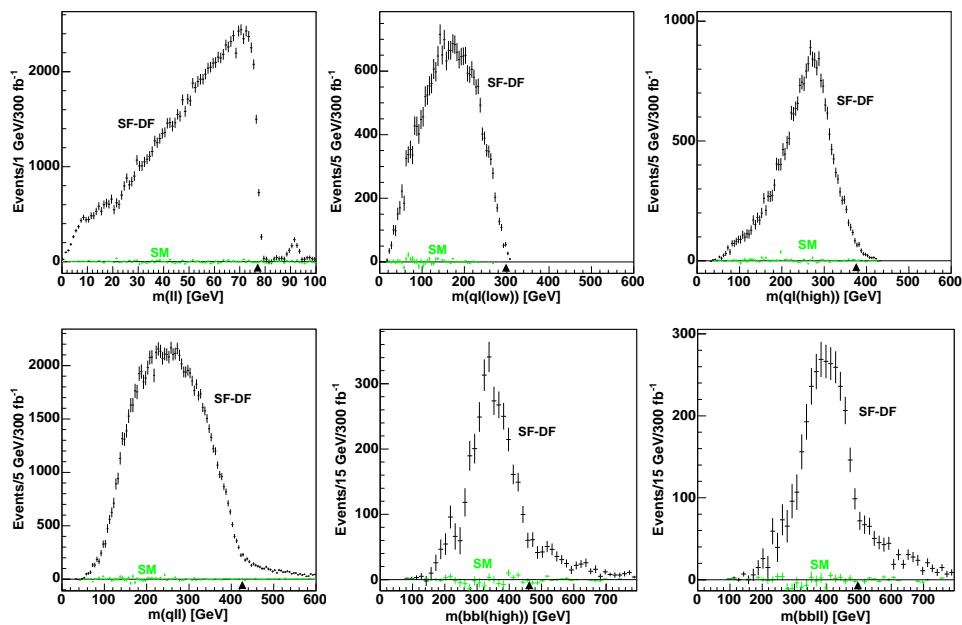


Figure 3: Some of the available experimental mass distributions for SPS 1a (α). The triangles mark the positions of the theoretical endpoints.

For the two SUSY scenarios reported on here, a selection of the available different-flavour-subtracted mass distributions (‘SF-DF’) are shown in Figs. 3 and 4. The plots are given for 300 fb^{-1} , which is attained after three years at design luminosity. The Standard Model part of the samples is plotted separately in green (‘SM’). Although the SM background is likely to be somewhat underestimated in these analyses, it is seen to have limited impact on the total distributions. The first four distributions of Fig. 3 correspond to the upper set of distributions in Fig. 2. While the experimental version of the m_{ql} distribution no longer resembles its theory counterpart, appropriate cuts amend this situation for the two m_{ql} distributions, although at the price of reduced statistics. The two last distributions are constructed from

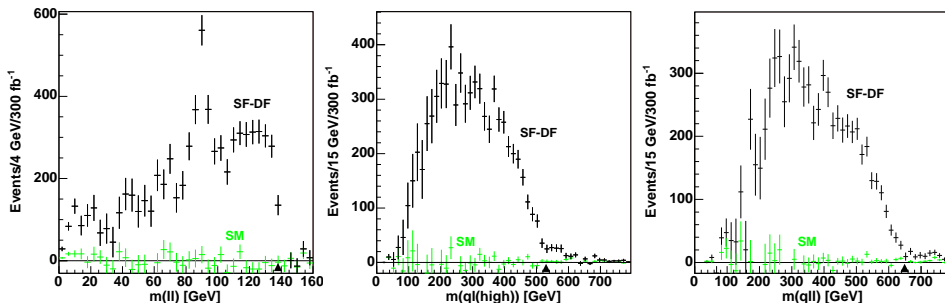


Figure 4: Some of the available experimental mass distributions for SPS 1a (β). The triangles mark the positions of the theoretical endpoints.

events with two b -tagged jets and access the gluino part of the decay chain, allowing for the determination of the gluino mass.

Although there are noticeable smearing and background effects in all the distributions, the edges are quite pronounced and point in the close vicinity of the theoretical endpoint. This is also true for the SPS 1a (β) distributions, where the signal cross-section is some 25 times lower. Measuring the distribution endpoints is in itself a troublesome task. Apart from the statistical uncertainty, there is a (yet) largely uncontrolled systematic error from the signal and background hypothesis made in the actual fitting. Attempts at improvement are being pursued, and will be much more so if SUSY is discovered at the LHC. In our investigation we have therefore taken the optimistic short-cut and assumed that this systematic error will be dominated by the controllable statistical and jet energy scale errors.

Furthermore, rather than obtaining the SUSY masses for the specific endpoint measurements found from the distributions in Figs. 3 and 4 as well as similar distributions not shown here, these endpoints, or more precisely their statistical errors, were used as indicative of what the LHC will be able to do, and an *ensemble* of typical LHC experiments was generated. For each experiment the SUSY masses were found from a numerical χ^2 fit. See [6, 10] for details.

While the endpoint measurements provide us with sufficient information to obtain the masses, inherent to the method are two complicating effects. First, the endpoints relate to *mass differences* much more than to the masses themselves, hence the errors on mass differences are much smaller than on the masses. For the lighter masses the precision for the two quantities can

typically differ by around an order of magnitude. This must be considered a limitation of the method, since what enters further application are usually the masses, not mass differences. The most familiar example is the input to the RGE equations which on the basis of the SUSY masses allow us to make statements on the GUT-scale physics [4]. Another example is cross-section considerations. Second, there is a high probability that several sets of masses give the same set of endpoints. If the number of masses is equal to the number of measured endpoints, this is exactly true. If more endpoint measurements are available, the system becomes overconstrained in favour of the correct solution, but due to measurement uncertainties, more than one solution must still often be considered. The relevant measure for comparing minima, is their difference in χ^2 value for the mass fit. If this difference is small, both minima are at the same level of compatibility with the endpoint measurements and must be accepted. In order to choose one rather than the other, more information is required than what the endpoints alone provide. (For a discussion of these ambiguities, see [12].)

In the case of SPS 1a (α) there are two competing solutions, the nominal one, which is in mass region $(1,1)^3$, and a second one in region $(1,2)$. If we accept solutions for which the difference in χ^2 down to the global minimum is less than 1 (3), there is a 12% (30%) probability that the system has two solutions. The probability that the nominal-region solution appears is very high, but there is a substantial admixture of the $(1,2)$ solution. In Table 1 the resulting masses for the two solution types are shown together with the nominal values (“Nom”). The masses are given first, then mass differences, with $m_{\tilde{\chi}_1^0}$ selected as reference point. The better precision of the mass differences is apparent, especially for the lighter masses.

In the case of SPS 1a (β) three minima are competing, the nominal solution, a second solution with similar masses and a third solution with much higher masses. Again, the nominal solution is available in most cases, but the admixture from the other one or two is significant. The preeminence of mass differences over masses, in terms of precision, is once more confirmed. Numbers can be found in [6].

Both the intrinsic “weaknesses” of the endpoint method discussed above involve an uncertainty of the SUSY mass scale. A Linear Collider measurement of the LSP mass effectively sets this scale, so combining the measurements from the LHC with those from a Linear Collider improves drastically the accuracy on the SUSY masses [15].

³See [6] for the definition of the mass regions.

Table 1: SPS 1a (α). Nominal masses, “Nom”, ensemble means, $\langle m \rangle$, and root-mean-square distances from the mean, σ , all in GeV.

	Nom	$(1,1)$		$(1,2)$	
		$\langle m \rangle$	σ	$\langle m \rangle$	σ
$m_{\tilde{\chi}_1^0}$	96.1	96.3	3.8	85.3	3.4
$m_{\tilde{l}_R}$	143.0	143.2	3.8	130.4	3.7
$m_{\tilde{\chi}_2^0}$	176.8	177.0	3.7	165.5	3.4
$m_{\tilde{q}_L}$	537.2	537.5	6.0	523.5	5.0
$m_{\tilde{g}}$	595.2	595.5	7.2	582.5	6.8
$m_{\tilde{l}_R} - m_{\tilde{\chi}_1^0}$	46.92	46.93	0.28	45.11	0.72
$m_{\tilde{\chi}_2^0} - m_{\tilde{\chi}_1^0}$	80.77	80.77	0.18	80.19	0.29
$m_{\tilde{q}_L} - m_{\tilde{\chi}_1^0}$	441.2	441.2	3.1	438.0	2.8
$m_{\tilde{g}} - m_{\tilde{\chi}_1^0}$	499.1	499.2	5.6	497.0	5.4

P. O. would like to thank the organizers of the *Southeastern European Workshop Challenges Beyond the Standard Model*, 19-23 May 2005, Vrnjacka Banja, Serbia for the invitation to a very interesting meeting. This work has been performed partly within the ATLAS Collaboration, and we thank collaboration members for helpful discussions. We have made use of the physics analysis framework and tools which are the result of collaboration-wide efforts. This research has been supported in part by the Research Council of Norway.

REFERENCES

- [1] P. Fayet and S. Ferrara, Phys. Rept. **32** 249 (1977); S. Dimopoulos and H. Georgi, Nucl. Phys. B **193** 150 (1981); H. P. Nilles, Phys. Rept. **110** 1 (1984); H. E. Haber and G. L. Kane, Phys. Rept. **117** 75 (1985).
- [2] K. Inoue, A. Kakuto, H. Komatsu and S. Takeshita, Prog. Theor. Phys. **68** (1982) 927 [Erratum-ibid. **70** 330 (1983)]; Prog. Theor. Phys. **71** 413 (1984); N. K. Falck, Z. Phys. C **30** 247 (1986); L. E. Ibanez and G. G. Ross, Phys. Lett. B **110** 215 (1982); L. E. Ibanez, Phys. Lett. B **118** 73 (1982); J. R. Ellis, D. V. Nanopoulos and K. Tamvakis, Phys. Lett. B **121** 123 (1983); L. Alvarez-Gaume, J. Polchinski and M. B. Wise, Nucl. Phys. B **221** 495 (1983).
- [3] H. Goldberg, Phys. Rev. Lett. **50** 1419 (1983); L. M. Krauss, Nucl. Phys. B **227** 556 (1983); J. R. Ellis, J. S. Hagelin, D. V. Nanopoulos, K. A. Olive and M. Srednicki, Nucl. Phys. B **238** 453 (1984).
- [4] B. C. Allanach, G. A. Blair, S. Kraml, H. U. Martyn, G. Polesello, W. Porod and P. M. Zerwas, arXiv:hep-ph/0403133.
- [5] A. H. Chamseddine, R. Arnowitt and P. Nath, Phys. Rev. Lett. **49** (1982) 970.
- [6] B. K. Gjelsten, D. J. Miller and P. Osland, JHEP **0412**, 003 (2004) [arXiv:hep-ph/0410303].
- [7] B. K. Gjelsten, D. J. Miller and P. Osland, JHEP **0506**, 015 (2005) [arXiv:hep-ph/0501033].
- [8] B. C. Allanach *et al.*, in *Proc. of the APS/DPF/DPB Summer Study on the Future of Particle Physics (Snowmass 2001)* ed. N. Graf, Eur. Phys. J. C **25** (2002) 113 [eConf **C010630** (2001) P125] [arXiv:hep-ph/0202233].

- [9] D. J. Miller, P. Osland, A. R. Raklev, Invariant mass distributions in cascade decays, CERN-PH-TH/2005-121, arXiv:hep-ph/0510356.
- [10] B. C. Allanach, C. G. Lester, M. A. Parker and B. R. Webber, *JHEP* **0009** (2000) 004 [arXiv:hep-ph/0007009].
- [11] H. Baer, C. h. Chen, F. Paige and X. Tata, *Phys. Rev. D* **53** (1996) 6241 [arXiv:hep-ph/9512383]; I. Hinchliffe, F. E. Paige, M. D. Shapiro, J. Soderqvist and W. Yao, *Phys. Rev. D* **55** (1997) 5520 [arXiv:hep-ph/9610544]; I. Hinchliffe, F. E. Paige, E. Nagy, M. D. Shapiro, J. Soderqvist and W. Yao, LBNL-40954; H. Bachacou, I. Hinchliffe and F. E. Paige, *Phys. Rev. D* **62** (2000) 015009 [arXiv:hep-ph/9907518]; G. Polesello, *Precision SUSY measurements with ATLAS for SUGRA point 5*, ATLAS Internal Note, PHYS-No-111, October 1997.
- [12] B. K. Gjelsten, D. J. Miller and P. Osland, arXiv:hep-ph/0507232.
- [13] T. Sjöstrand, P. Edén, C. Friberg, L. Lönnblad, G. Miu, S. Mrenna, E. Norrbin, *Comput. Phys. Commun.* 135 (2001) 238; T. Sjöstrand, L. Lönnblad and S. Mrenna, “PYTHIA 6.2: Physics and manual”, arXiv:hep-ph/0108264.
- [14] E. Richter-Was, D. Froidevaux and L. Poggioli, “ATLFAST 2.0: a fast simulation package for ATLAS”, Tech. Rep. ATL-PHYS-98-131 (1998)
- [15] G. Weiglein *et al.* [LHC / ILC Study Group], arXiv:hep-ph/0410364.